analytical chemistry

Article

pubs.acs.org/ac

Biofunctionalized Gold Nanoparticles for Colorimetric Sensing of Botulinum Neurotoxin A Light Chain

Xiaohu Liu, Yi Wang, Peng Chen, Yusong Wang, Jinling Zhang, Daniel Aili,*,† and Bo Liedberg*

Centre for Biomimetic Sensor Science, Nanyang Technological University, 50 Nanyang Drive, Singapore 637553, Singapore

Supporting Information

ABSTRACT: Botulinum neurotoxin is considered as one of the most toxic food-borne substances and is a potential bioweapon accessible to terrorists. The development of an accurate, convenient, and rapid assay for botulinum neurotoxins is therefore highly desirable for addressing biosafety concerns. Herein, novel biotinylated peptide substrates designed to mimic synaptosomal-associated protein 25 (SNAP-25) are utilized in gold nanoparticle-based assays for colorimetric detection of botulinum neurotoxin serotype A light chain (BoLcA). In these proteolytic assays, biotinylated peptides serve as triggers for the aggregation of gold nanoparticles, while the cleavage of these peptides by BoLcA prevents nanoparticle aggregation. Two different assay strategies are described, demonstrating limits of detection ranging from 5 to 0.1 nM of BoLcA with an overall assay time of 4 h. These hybrid enzyme-responsive nanomaterials provide rapid and sensitive detection for one of the most toxic substances known to man.

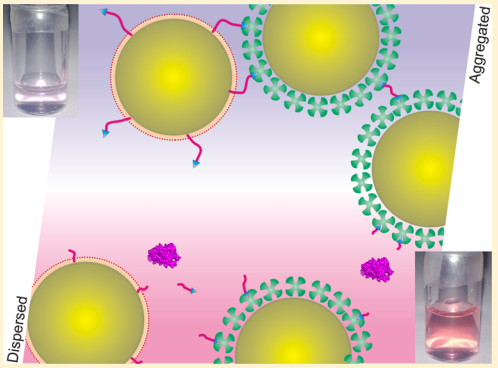

Botulinum neurotoxins (BoNTs) are produced by *Clostridium botulinum* and are classified into seven serotypes designated from A to G,[1] each of which comprises a 100 kDa heavy chain (HC) and a 50 kDa light chain (LC) linked via a disulfide bond. The HC contains a binding domain and a translocation domain, whereas the LC possesses a catalytic domain responsible for the proteolytic function.[2] The HC is generally considered as a transport vehicle that specifically targets the axon termini via the binding domain and enters the neurons through receptor-mediated endocytosis.[3] The translocation domain of HC mediates the escape of the LC from the endocytic vesicle to the cytoplasm.[4] The LC proteolytically degrades components of SNARE (soluble *N*-ethylmaleimide-sensitive-factor attachment protein receptor) proteins, which prevents neurotransmitters from being released into the synaptic gap of the neuromuscular junctions. As a consequence, the subsequent muscle suffers from flaccid paralysis.[5] BoNT therefore causes a serious and life-threatening illness (botulism).[1] It is considered one of the most neurotoxic substances known with an estimated lethal dose of 1.3−13 ng/kg, depending on the different methods of exposure, such as injection and inhalation.[6] In addition to being a food pathogen, BoNT is also a potential bioterror weapon.[7] Hence, there is a great need for accurate and rapid assays for botulinum neurotoxins.

Currently, the standard method for detection of BoNT is the mouse bioassay in which the symptoms of botulism are observed 2−4 days after the animals have been injected with a BoNT containing sample.[8] Alternative methods for BoNT detection include immunoassays.[8] Although these assays have demonstrated very low limit of detections (LODs), in the subpicomolar range, they tend to be slow, labor intensive, and provide little, if any, information about the enzymatic activity of BoNT.

By rational design of peptides containing a BoNT cleavage site, it is possible to obtain substrates specific for each serotype LC of BoNTs as each of them has a very specific recognition sequence.[9] Those peptide-based BoNT substrates have been used in combination with mass spectroscopy, surface plasmon resonance, Förster resonance energy transfer, and electrochemical luminescence for monitoring the activity and concentration of BoNT.[8,10−13] Unfortunately, most of these methods require highly advanced and expensive equipment.

Gold nanoparticles (AuNPs) have been extensively employed in bioanalytical applications. Different sizes and geometries of AuNPs, functionalized by proteins, peptides, and oligonucleotides, enable novel sensing strategies for highly sensitive and robust detection of biomolecules and biomolecular interactions.[14−16] The optical properties of AuNPs offer possibilities to transduce molecular interactions into readily detectable colorimetric signals that can be recorded by standard laboratory equipment and sometimes even by the naked eye.[17] The excitation of collective electron oscillations on the nanoparticle surface gives rise to a very pronounced extinction band in the visible wavelength regime. This localized surface plasmon resonance (LSPR) band is sensitive to local changes in refractive index and the aggregation/dispersion state of the nanoparticles. Particle aggregation typically results in a distinct red shift of the LSPR band. Recently, peptide-functionalized

Received: August 19, 2013
Accepted: February 3, 2014
Published: February 3, 2014

   dx.doi.org/10.1021/ac402626g | *Anal. Chem.* 2014, 86, 2345−2352

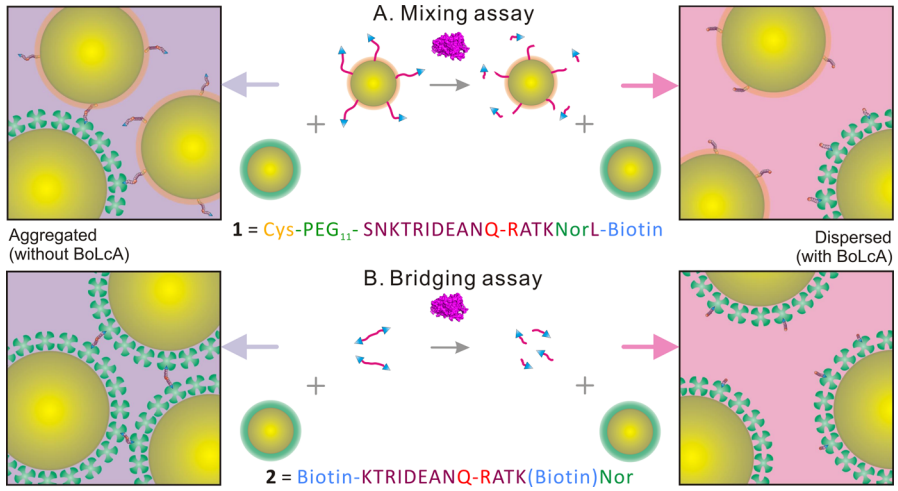

Figure 1. (A) Mixing and (B) bridging assays for detection of BoLcA using two peptide designs (**1** and **2**) and biofunctionalized AuNPs.

AuNPs have been utilized for colorimetric sensing of metal ions,[18,19] proteins,[20−22] and toxins.[23−26] Designed peptides are excellent candidates as synthetic receptors because they are more robust than proteins (e.g., antibodies) and provide enormous flexibility and versatility with respect to structural and chemical properties. Moreover, peptides are generally much smaller than proteins which, when used in combination with AuNPs, result in smaller particle separation upon particle aggregation and thus a more pronounced optical shift.[17]

In this paper, a rapid and robust colorimetric assay for BoNT serotype A light chain (BoLcA) is demonstrated. For peptides containing a BoLcA recognition/cleavage site, the proteolytic digestion by BoLcA drastically alters the aggregation pattern of the particles, which enables the concentration of active BoLcA to be determined. Two different assay strategies have been developed, using two different peptide designs (Figure 1). Peptide **1** includes an anchor (thiol group), a spacer (PEG), the recognition/cleavage site (peptide itself), and a terminal biotin. Peptide **2**, on the other hand, has the recognition/cleavage site inserted between two biotins. In strategy A (mixing assay), AuNPs are functionalized with the designed biotinylated-peptides (**1**-AuNPs) that aggregate with neutravidin-functionalized AuNPs (navi-AuNPs). In strategy B (bridging assay), aggregation of navi-AuNPs is induced by a bridging of the nanoparticles using the bibiotinylated peptide **2**. These assays demonstrate LODs ranging from (A) 5 nM down to (B) 0.1 nM of BoLcA.

EXPERIMENTAL SECTION

Materials. The modified peptide substrates Cys-PEG_{11}-SNKTRIDEANQRATKNorL-biotin (**1**) and biotin-KTRIDEANQRATK(biotin)Nor (**2**) were purchased from the Peptide Synthesis Core Facility, School of Biological Sciences, Nanyang Technological University. Singapore. The peptides were synthesized on the solid phase, identified using matrix-assisted laser desorption/ionization-time-of-flight (MALDI-TOF) mass spectrometry and purified by high-performance liquid chromatography (HPLC). Botulinum neurotoxin serotype A light chain (BoLcA), SNAPtide, and unquenched calibration peptide for SNAPtide were purchased from List Biological Laboratories, Inc. PEG_7 thiol acid [*O*-(2-carboxyethyl)-*O*′-(2-mercaptoethyl)-heptaethylene glycol] was purchased from Polypure AS, Norway. Neutravidin was purchased from Thermo Fisher Scientific Inc. Other chemicals were purchased from Sigma-Aldrich without further purification. Gold nanoparticles with an approximate average diameter of 20 nm were prepared by citrate reduction of $HAuCl_4$. Briefly, 12 mL of $HAuCl_4$ (2.54 mM) was added to 102 mL of pure water (Milli-Q, 18.2 MΩ cm) under stirring and brought to a boil in a round-bottom flask with a condenser to maintain a constant volume of the reaction mixture. Upon boiling, 6 mL of 10 mg/mL sodium citrate was added and left to continue boiling for another 30 min under stirring, until the solution turned red. Gold nanoparticles with an approximate average diameter of 28 nm were synthesized by the same method with a lower reaction temperature (60 °C).

Peptide Functionalization of AuNPs (1-AuNP). PEG_7 thiol acid (aPEG) was mixed with the peptide substrate (**1**) at different concentration ratios, ranging from 0.004 to 0.02 (**1**:aPEG) in 500 μL of 50 mM HEPES [4-(2-hydroxyethyl)-1-piperazineethanesulfonic acid] buffer (pH 7.4, 0.05% Tween 20) followed by addition of an equivalent volume of 20 nm AuNPs (0.5 nM) and incubated for 2 h. The final concentration of the aPEG molecules was 25 μM. The AuNPs were repeatedly centrifuged and resuspended in fresh 50 mM HEPES buffer, until the estimated free peptide concentration in the solution was less than 1 pM. The purified AuNPs were concentrated to 5 nM and stored at 4 °C until use.

Neutravidin Functionalization of AuNPs (navi-AuNPs). AuNPs (20 and 28 nm) were modified with neutravidin by incubation of 500 μL of AuNPs (0.5 and 0.18 nM, respectively) with 100 μL of 1 mg/mL neutravidin in 400 μL of 20 mM carbonate buffer (pH 10) for 2 h. Unbound neutravidin was removed by repeated centrifugation, and particles were resuspended in fresh carbonate buffer (pH 10) until the estimated concentration of free neutravidin in solution was less than 1 pM. Finally, the neutravidin modified AuNPs were resuspended in 50 mM HEPES buffer.

Mass Spectrometry. BoLcA was added into the synthetic peptides solution in a 50 mM HEPES buffer, pH 7.4, with 0.05% Tween 20 to achieve final concentrations of 20 nM BoLcA and 10 μM peptide substrates followed by incubation at 37 °C for 3 h. The enzymatic reaction was terminated by heating to 80 °C. The reaction solution was desalted using reversed phase ZipTip (Merck Millipore, Germany) prior to analysis by MALDI-TOF mass spectrometry.

dx.doi.org/10.1021/ac402626g | *Anal. Chem.* 2014, 86, 2345−2352

Analysis of BoLcA Proteolytic Activity with SNAPtide. For the calibration analysis, freshly prepared 1 μM solution of unquenched calibration peptide in 50 mM HEPES buffer was further diluted into appropriate wells of 96-well plate (Corning) to make the final amount (from 0 to 0.2 nmoles). For the SNAPtide cleavage assay, 0.5 nmoles of SNAPtide in a 50 mM HEPES buffer was added into wells and reactions began with the addition of 8.3 nM of BoLcA at 37 °C. The data from the calibration and cleavage assays were collected using a Tecan Infinite M200 Pro Plate Reader (Tecan, Research Triangle Park, NC) in the kinetic mode in which the excitation and emission wavelengths were set as 490 and 523 nm, respectively.

Detection of BoLcA by Colorimetric Gold Nanoparticle Assays. In the mixing assay (Figure 1A), various concentrations of BoLcA spiked in the HEPES buffer were incubated with 10 μL of **1**-AuNPs (5 nM) at 37 °C for 20 h. The reaction was terminated by heating to 80 °C, and the solution was diluted 10 times with a 50 mM HEPES buffer. UV−Visible (UV−Vis) spectra were recorded immediately after mixing the reacted **1**-AuNPs and navi-AuNPs (100 μL of each, 20 nm, 0.25 nM) with 2 min intervals for 90 min. Negative control (aPEG-AuNPs) and blank control (**1**-AuNPs without BoLcA preincubation) were performed in the same way. In order to test the influence of immobilization of **1** on the accessibility of BoLcA to hydrolyze **1**, various concentrations of **1** (0.1−10 μM) were incubated with BoLcA prior to immobilization on AuNPs. Subsequently, the BoLcA treated **1**-AuNPs were mixed with navi-AuNPs in the same way as above. UV−Vis spectra were obtained after 90 min. In the peptide bridging assay (Figure 1B), **2** was incubated with various concentrations of BoLcA in the HEPES buffer at 37 °C for 3 h followed by addition of purified navi-AuNPs (28 nm, 0.18 nM). UV−Vis spectra were recorded immediately after mixing with 2 min intervals for 30 min.

RESULTS AND DISCUSSION

Peptide Design. Intensive work has been carried out in order to reveal the substrate requirements for BoNT serotype A (BoNT/A).[27,28] It has been found that a short peptide derived from the C-terminal end (187−203) of the SNAP-25 protein can be hydrolyzed by BoNT at a similar rate as the full length SNAP-25, as long as the peptide has a minimum length of 14 to 16 amino acids (i.e., 9 to 11 residues on the carboxyl-terminal side of the cleaving amide bond and 5 on the amino-terminal side) and the P1′ site of arginine is retained.[28] Extensive interactions (e.g., hydrophobic side-chain interactions, polar side-chain, and backbone contacts) between the short peptide substrate and BoLcA have been confirmed.[29] Notably, a β-exosite present at the C-terminus of the peptide substrate has been reported to significantly improve both the substrate-enzyme binding affinity and the catalytic rate.[29] The β-exosite is separated from the cleavage site by 2 residues and forms a β-sheet together with the "250 loop", which is a region encompassing residue 242−259 of BoLcA.

With this in mind, two synthetic peptide substrates were designed (**1** and **2**). The sequence of peptide **1** is based on the 17 amino acids at the C-terminus of SNAP-25 protein (187−203) as indicated in Figure 1A but with methionine (M) in position 202 replaced by norleucine (Nor). The substitution of M with Nor previously has been found to increase the proteolytic rate of BoLcA.[27] At the same time, it prevents the potentially problematic interaction between the AuNPs and the sulfur-containing side chain of methionine. This 17 amino acid peptide contains all the BoLcA, recognizing residues that are close to the cleavage site, including a β-exosite at the C-terminus. The amide bond between glutamine and arginine (Q-R) located in the middle of the target peptide is the cleavage point for BoLcA proteolysis, as indicated in Figure 1. The proteolytic cleavage of **1** by BoLcA at this position was confirmed using MALDI-TOF. After a 3 h incubation of **1** with BoLcA at 37 °C, two peaks appeared corresponding to the N-terminal half of **1** (m/z = 1977) and the C-terminal half (m/z = 1055) (Figure S-1 of the Supporting Information).

Peptide **1** was designed to be immobilized directly on AuNPs via a thiol moiety at the N-terminal Cys residue. The BoLcA recognition sequence was separated from the Cys residue by an 11-unit ethylene glycol oligomer in order to minimize steric hindrance caused by immobilization to the AuNPs. A biotin group was attached to the C-terminal in order to enable specific aggregation when exposed to neutravidin-functionalized AuNPs (navi-AuNPs).

Peptide **2** (Figure 1B) shared 14 of the core amino acids of **1** but was modified with two biotin moieties, one at each terminus. The two biotins were incorporated to facilitate specific supramolecular cross-linking of navi-AuNPs.

Surface Functionalization of Gold Nanoparticles. In order to increase the colloidal stability of the peptide-modified AuNPs and to allow tuning of the peptide surface concentration, **1** was co-immobilized with PEG_7 thiol acid (aPEG). Solutions with various molar ratios of **1** and aPEG (**1**:aPEG), ranging from 0.004 to 0.02, were investigated. The UV−Vis spectra showed a minor peak shift of the LSPR band from 520 to 522 nm (Figure 2a). The surface functionalization of the AuNPs with the thiolated molecules was expected to result in a mixed monolayer of **1**:aPEG with an approximate film thickness of 4 nm, which was confirmed by the observed 2 nm shift ($\Delta\lambda$) of the LSPR band. Calculations based on the model reported by Read et al.[30] using a penetration depth (l_p) equal to 20 nm and n = 1.45, yielded $\Delta\lambda$ = 1.8 nm, which was in good agreement with the experimental observations. (For a brief introduction to the method proposed by Read et al., see Text S-1 of the Supporting Information.) The modified particles, **1**-AuNPs, were highly stable at molar ratios of **1**:aPEG < 0.02. The number of immobilized peptides per nanoparticle was estimated based on the assumption that the binding affinities of **1** and aPEG to the gold particles (d = 20 nm) were equal and that each molecule would occupy a surface area of 0.2 nm^2. Accordingly, the number of **1** on each AuNP at a ratio of **1**:aPEG = 0.01 was about 63 peptides (Table S-1 of the Supporting Information).

The 20 nm AuNPs showed a 5 nm red shift of the LSPR band after functionalization with neutravidin (Figure 2b) because of the increase in refractive index upon protein adsorption. Furthermore, an increase in particle size from 20 nm (size of the citrate stabilized AuNPs) to an average of 26 nm in diameter after the modification with neutravidin was observed using dynamic light scattering (Figure S-2 of the Supporting Information). These results are reasonable, since the 60 kDa neutravidin is a globular protein with a diameter around 3−4 nm. Neutravidin has an isoelectric point (pI) of 6.3, and the adsorption was carried out at pH 10 to prevent unspecific charge-induced bridging aggregation of the citrate-capped AuNPs. The adsorption of neutravidin to gold was facilitated by both hydrophobic interactions and formation of covalent bonds by thiol groups present in Cys residues on the protein surface.[31]

dx.doi.org/10.1021/ac402626g | Anal. Chem. 2014, 86, 2345−2352

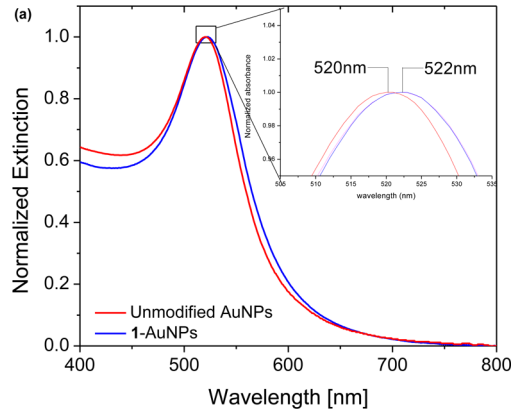

Figure 2. (a) Normalized extinction spectra of AuNPs (red) and **1**-AuNPs (blue). Inset: zoom-in of the LSPR peak shift. (b) Normalized extinction spectra of AuNPs (red) and navi-AuNPs (blue).

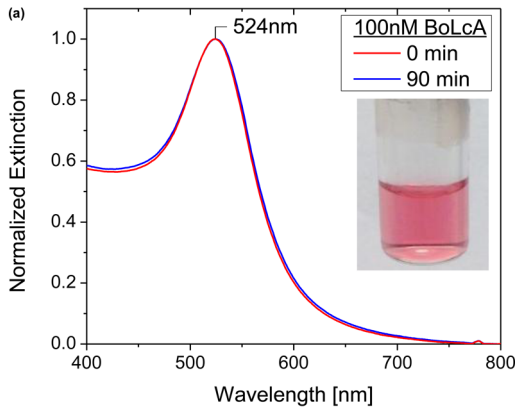

Figure 3. Normalized extinction spectra of the mixture solution of navi-AuNPs and **1**-AuNPs which was preincubated with (a) 100 nM BoLcA and without (b) BoLcA (as control). Inset: photographs of AuNP solutions.

Colorimetric Particle-Mixing Assays of BoLcA. AuNPs modified with only aPEG (aPEG-AuNPs) demonstrated excellent colloidal stability. Incubating aPEG-AuNPs with navi-AuNPs did not induce any detectable changes in the LSPR band, indicating that no significant attractive interactions exist between the aPEG-AuNPs and navi-AuNPs. However, the **1**-AuNPs showed more than a 20 nm red shift of the LSPR band after addition of navi-AuNPs, resulting in a partial precipitation (Figure S-3 of the Supporting Information). The presence of the biotinylated peptide **1** on the AuNPs was thus critical for inducing particle aggregation. The LSPR shift was saturated within 1−2 h, which was slower than the kinetics of the biotin-neutravidin interaction in solution.[32] This could be ascribed to the slow diffusion and relatively low collision frequency of the AuNPs, as well as the accessibility of the biotin moiety to the immobilized neutravidin. In the mixing assay, the peptide-modified particles were first incubated with BoLcA (direct assay), before addition of navi-AuNPs. After a 20 h incubation of **1**-AuNPs (**1**:aPEG = 0.01) with 100 nM BoLcA, no shift of the LSPR peak was obtained upon addition of navi-AuNPs (Figure 3a). In addition, transmission electron microscope (TEM) images primarily showed dispersed particles (Figure S-4a of the Supporting Information), strongly suggesting that the proteolytic cleavage of **1** by BoLcA, excised the C-terminal biotin group in **1**, which prevented the specific association with navi-AuNPs. In contrast, a shift from 525 to 548 nm ($\Delta\lambda$ = 23 nm) was observed for the **1**-AuNPs not exposed to BoLcA prior to addition of navi-AuNPs (Figure 3b), which was confirmed by the presence of large particle aggregates in the TEM image (Figure S-4b of the Supporting Information). The dramatic difference in the LSPR band of **1**-AuNPs could be clearly observed by the naked eye (Figure 3 inset) as a pronounced difference in color with and without incubation of 100 nM BoLcA.

In order to optimize the sensor response, AuNPs were modified in solutions containing different molar ratios of **1** and aPEG ranging from 0.004 to 0.02. As shown in Figure 4a, the extent of the LSPR peak shift after addition of navi-AuNPs ($\Delta\lambda_c$) increased when increasing the relative amount of **1**. Maximum aggregation was achieved at a molar ratio of **1**:aPEG > 0.01 (black line, Figure 4a). The optical shift when first exposing **1**-AuNPs to BoLcA ($\Delta\lambda_s$) varied for the different ratios of **1**:aPEG (100 nM BoLcA, 20 h incubation). The sensor response ($\Delta\lambda_r$) is defined as the difference between the LSPR peak shifts with and without BoLcA treatment (i.e., $\Delta\lambda_r = \Delta\lambda_c - \Delta\lambda_s$).

A very low response $\Delta\lambda_r$ was obtained for ratios of **1**:aPEG > 0.02 and <0.004, whereas substantial responses were seen for **1**:aPEG ratios between 0.004 and 0.02, peaking at around 0.01 (broken blue line, Figure 4a). At a low surface concentration of **1**, the low number of biotins on each particle limited the probability for aggregation by navi-AuNPs. At a high surface concentration of **1**, there was on the other hand extensive particle aggregation upon exposure to navi-AuNPs, as a large fraction of these peptides had to be hydrolyzed by BoLcA in order to produce a significant sensor response. Accordingly, the **1**:aPEG ratio of 0.01 was considered as optimal, providing a maximum sensor capacity and sensitivity for BoLcA detection. The sensor response for concentrations of BoLcA ranging from

dx.doi.org/10.1021/ac402626g | Anal. Chem. 2014, 86, 2345−2352

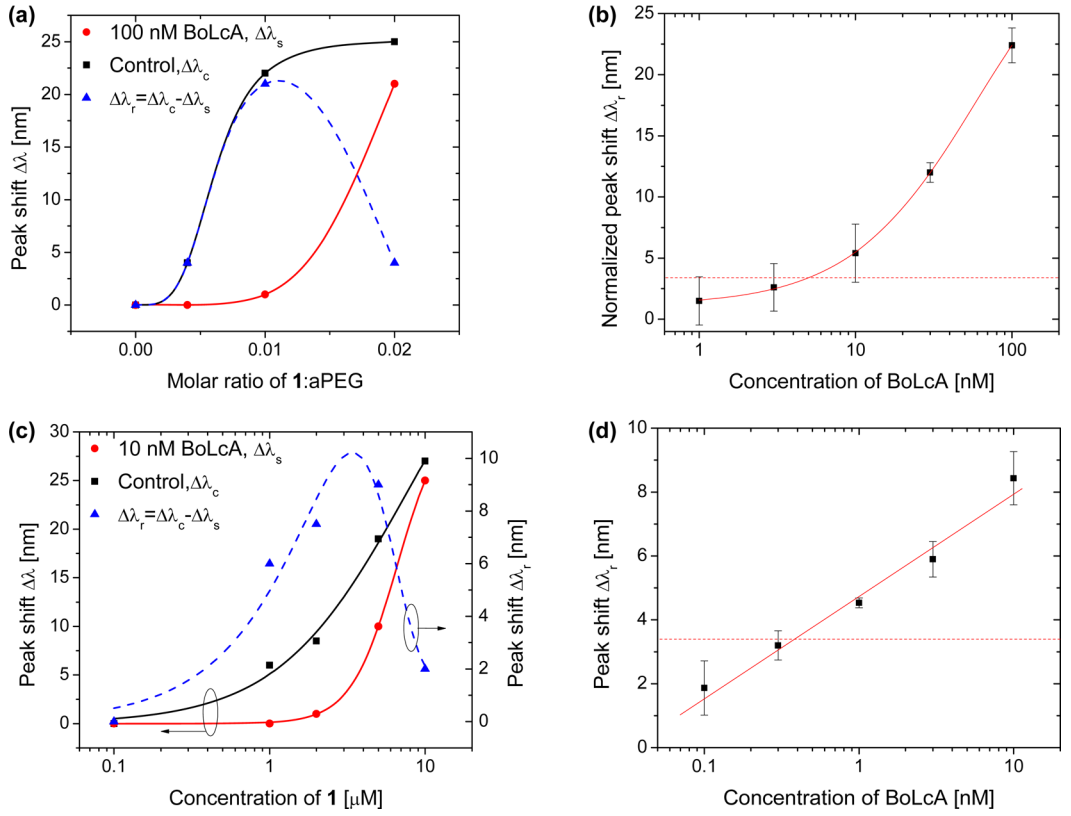

Figure 4. (a) Comparison of LSPR peak shifts induced by different molar ratios of **1** and aPEG-functionalized AuNPs after mixing with navi-AuNPs. Controls ($\Delta\lambda_c$) (■); samples preincubated with 100 nM BoLcA ($\Delta\lambda_s$) (red ●); sensor response ($\Delta\lambda_r$) (blue ▲). (b) Calibration curve for the peak shifts as a function of the BoLcA concentrations by the direct assay. (Error bars are the standard error of the mean, $n \geq 3$.) (c) Comparison of LSPR peak shifts induced by different concentrations of **1**. Controls ($\Delta\lambda_c$) (■); **1** incubated with 10 nM BoLcA for 3 h prior to immobilization on AuNPs and addition of navi-AuNPs ($\Delta\lambda_s$) (red ●); sensor response ($\Delta\lambda_r$) (blue ▲). (d) Calibration curve for the peak shifts as a function of the BoLcA concentrations by the indirect assay. (Error bars are the standard error of the mean, $n \geq 3$.)

1 to 100 nM is shown in Figure 4b. The LOD for the detection of BoLcA was estimated to be 5 nM, which was equal to the concentration of BoLcA at which the sensor response was 3× the standard deviation of the control experiments.

This strategy, however, suffered from a relatively long assay time, typically requiring 20 h of incubation of **1**-AuNPs with the BoLcA sample in order to provide a large enough sensor response. Furthermore, it has been known that the active site of BoLcA is buried rather deep inside the protein (ca. 2.4 nm).[33] Thus, steric constraints induced by the AuNP might affect the accessibility of BoLcA to the cleavage site of **1**, although the peptide was attached to gold via a long oligo(ethylene glycol) spacer. The flexibility of the long spacer could potentially also allow for conformations/orientations of **1** that were unfavorable for hydrolysis.[13] Additionally, the short peptide substrate might not be as efficiently recognized by BoLcA as the whole SNAP-25 protein,[34] and the N-terminal spacer group on **1** might reduce the specificity for catalytic cleavage of BoLcA. It should be stressed that the catalytic rate constant k_{cat} of BoLcA measured with the standard SNAPtide was estimated as 22.6 per hour (Figure S-5 of the Supporting Information), which was significantly lower than previously reported,[11] indicating that the BoLcA utilized here did not display as high an activity as other BoNT proteases.[1]

In order to better understand the steric constraints caused by immobilization, peptide **1** was incubated with BoLcA prior to immobilization on the AuNPs (indirect assay). Ten nanomolar BoLcA was incubated with **1** (0.1−10 μM) for 3 h prior to addition of citrate-capped AuNPs (0.5 nM) and aPEG (**1**:aPEG = 0.003). The **1**-AuNPs were incubated for 2 h and purified by repeated centrifugations. UV−Vis spectra were subsequently obtained after 2 h mixing of the **1**-AuNPs with the navi-AuNPs. Significantly more aggregation was observed without BoLcA treatment (Figure 4c). The sensor response $\Delta\lambda_r$ (broken blue line) showed a similar trend as the direct method described above, with a maximum response at 2−4 μM of free **1**. An LOD of 0.4 nM BoLcA was subsequently obtained by using 3 μM of peptide **1** (Figure 4d).

Despite using a significantly shorter incubation time (3 h), the 10-fold higher sensitivity obtained when exposing **1** to BoLcA prior to immobilization highlighted the strong negative influence of immobilization on the accessibility of the peptide to enzymatic hydrolysis.

The activity of BoLcA on free **1** was estimated under the assumption that uncleaved **1** would induce AuNPs aggregation accordingly. Figure 4c showed 0.9 nm of peak shift ($\Delta\lambda_s$) at 2 μM of **1**, which was about 10% of the control peak shift ($\Delta\lambda_c$) = 8.5 nm, indicating that ∼90% of **1** was proteolyzed by 10 nM BoLcA. Accordingly, the rate of cleavage k_{cat} was estimated as 69 ± 10 per hour, which was about 3-fold better than the standard SNAPtide assay (Figure S-5 of the Supporting Information). This might be due to a longer recognition sequence of **1**, and the better design of the sequence (for instance the replacement of M with Nor) as compared to SNAPtide.

dx.doi.org/10.1021/ac402626g | *Anal. Chem.* 2014, 86, 2345−2352

Colorimetric Peptide-Bridging Assay of BoLcA. In order to circumvent the problems imposed by the immobilization of **1**, a second peptide (**2**) was designed. Peptide **2** was incorporated with two biotin moieties [biotin-KTRIDEANQ-RATK(biotin)Nor], thus capable of bridging navi-AuNPs, unless hydrolyzed (Figure 1B). Addition of **2** to navi-AuNPs caused a concentration-dependent red shift of the LSPR band, saturating at about $\Delta\lambda_c$ = 17.5 nm for 75 nM of peptide **2** after a 30 min incubation (Figure 5a). The sigmoidal shape of the response curve suggested a certain amount of unspecific interactions. If the aggregation were induced solely by the biotin-mediated binding, a bell-shape curve would be expected, since neutravidin-binding sites would be saturated at high concentrations, preventing aggregation.

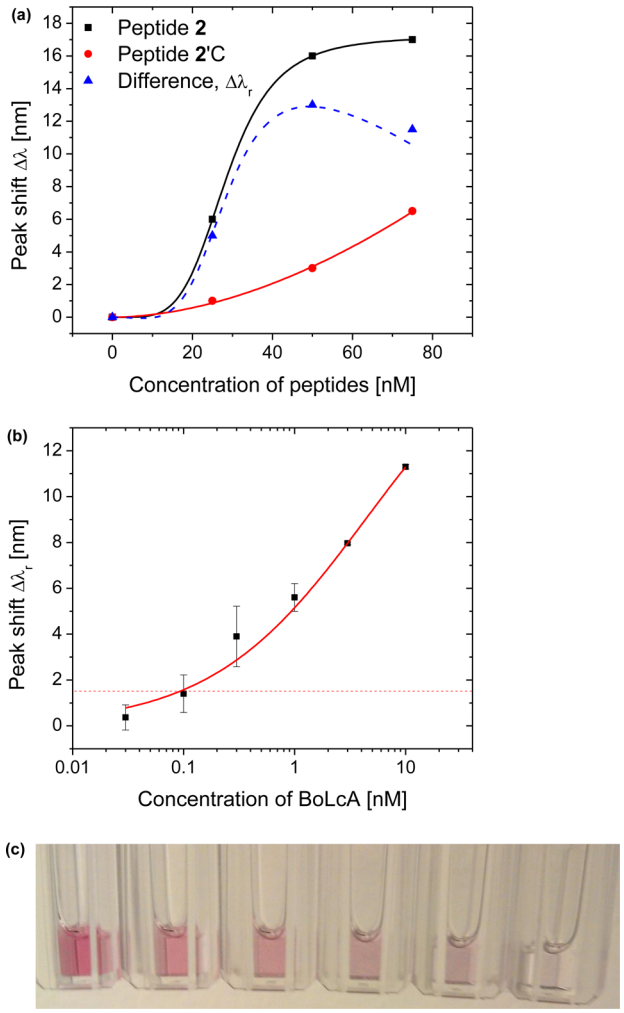

Figure 5. (a) Comparison of LSPR peak shifts induced by different concentrations of **2** (■) and **2**′C (red ●) incubated with navi-AuNPs. The blue ▲ show the peak-shift differences ($\Delta\lambda_r$) between **2** and **2**′C. (b) Calibration curve for the peak shifts as a function of the BoLcA concentrations by the bridging assay. (Error bars are the standard error of the mean, $n \geq 3$.) (c) Photograph of the navi-AuNP solutions after mixing against **2**, preincubated with 10, 3, 1, 0.3, 0.1, and 0 nM of BoLcA.

This was further confirmed by addition of the C-terminal half of **2** [**2**′*C* = RATK(biotin)Nor], that mimicked the C-terminal product after hydrolysis of **2** by BoLcA. Partial aggregation of navi-AuNPs was observed at a high concentration of **2**′C (75 nM), as indicated in the peak shift ($\Delta\lambda_s$) = 7 nm (red line, Figure 5a). This aggregation was presumably caused by the combination of the biotin and the positive net-charge of **2**′C that could induce unspecific bridging aggregation of the slightly negatively charged navi-AuNPs (*p*I of navi is 6.3). The second product [i.e., the N-terminal of the peptide (**2**′*N* = Biotin-KTRIDEANQ)] has a negative net charge and thus showed no observable peak shift upon incubation with navi-AuNPs. The aggregation of navi-AuNPs induced by **2** could therefore be due to both a specific and a minor amount of unspecific interactions. The peak-shift difference, $\Delta\lambda_r = \Delta\lambda_c - \Delta\lambda_s$, showed a maximum response at the peptide concentration of 50 nM (broken blue line, Figure 5a), which was the concentration used in further experiments for detection of BoLcA. An inverse relationship was found between the LSPR peak shift and the amount of BoLcA upon addition of the pre-BoLcA-incubated **2** to navi-AuNPs. The concentration-dependent peak shift ($\Delta\lambda_r$) and color changes are shown in Figure 5 (panels b and c), respectively. The LOD was found to be 0.1 nM (5 ng/mL of BoLcA), which is 50 times lower as compared to the direct assay based on peptide **1** (Table S-2 of the Supporting Information). This lower LOD is most likely the result of using a non-immobilized substrate in combination with a strategy where a relatively limited number of peptides had to be cleaved in order to affect the aggregation characteristics. Moreover, the bridging assay provided a 3-fold better LOD than a previously reported quantum-dot-based FRET method with LOD ~ 350 pM and assay time of 2−3 h.[13] It also provided a comparable LOD as compared to the antibody-based SPR sandwich assay (LOD of 1 ng/mL and assay time of 1−2 h)[35] but worse LOD as compared to the mouse lethality assay (LOD of 20−30 pg/mL and assay time of 2−4 days),[36] antibody-based ELISA (LOD of 0.2−2 ng/mL and assay time of 4 h),[37,38] and aptamber-based electrochemical assay (LOD of 40 pg/mL and assay time of 24 h).[39] The LOD demonstrated here is estimated to 5 ng/mL for BoLcA (MW 50 kDa), which, upon assuming that the catalytic activity is the same for BoLcA and BoNT/A, corresponds to 15 ng/mL for the intact toxin BoNT/A (MW 150 kDa). Although the lethal dose is not known for humans, it can be estimated from investigations on primates. For a person with a body weight of 60 kg, the lethal dose varies between 70 to 130 ng by injection (intravenously or intramuscularly), 600 to 800 ng (via inhalation), and 60 μg (orally).[6] For oral intake, 60 μg of BoNT/A in a volume of 100 mL corresponds to 600 ng/mL; that exceeds our LOD by a factor of 40. For a baby (5 kg), the corresponding calculation (in 100 mL) gives a lethal dose of about 50 ng/mL, which is still above our estimated LOD. For injection of 0.1 mL, which is the typical volume used in cosmetic applications, the concentration of BoNT/A is also around 700 ng/mL for a lethal dose of 70 ng. Thus, the LOD of our assay is below, and in some cases even well below the lethal concentrations of BoNT/A. It should also be noted that the bridging assay only requires one step after exposure to the sample, resulting in a relatively short assay time of 4 h.

We have in this manuscript compared two assays for detection of BoLcA, and discussed their respective pros and cons. Although, it is generally advisable to test new sensor technologies and assays under real conditions before making too far reaching conclusion about the overall performance, it is not within the scope of the current study to validate the assays in more complex environments. However, we are currently exploring strategies to test our assays in complex matrices by

dx.doi.org/10.1021/ac402626g | *Anal. Chem.* 2014, 86, 2345−2352

repeating the experiments in milk, honey, tap water, etc. We are also exploiting different assay formats and carriers for field applications to be published separately.

There are indeed several obstacles to account for when employing aggregation assays based on AuNPs in complex solutions because of uncontrolled adsorption of unknown substances onto the surfaces of the AuNPs. The particles may aggregate due to a variety of reasons and cause false negatives. The AuNP surfaces may also be blocked by proteins, thereby preventing the specific peptide(biotin)-neutravidin interactions to occur. The bridging assay using peptide **2**, however, offers an opportunity to reduce the above obstacles, as it minimizes the exposure of the AuNPs to complex solutions. Moreover, the simplicity of the assays and the use of robust molecular components (peptides) offer an attractive route for production of cheap assays with long shelf life for applications in field tests in resource-limited countries.

CONCLUSIONS

Peptides are attractive candidates for biomolecular recognition instead of protein-based receptors (e.g., antibodies). They offer comparable selectivity, in combination with high robustness. As reported here, peptide substrates (**1** and **2**) were designed and successfully employed for the detection of BoLcA by using a colorimetric colloidal gold reporter system. Biotinylated peptides served as the trigger for the aggregation of AuNPs. The presence of BoLcA induced the cleavage of the biotin parting from the peptide, thus keeping the AuNPs dispersed. In strategy A, the surface-based direct detection method showed an LOD of 5 nM, while the solution-based indirect detection by preincubation of the free peptide with BoLcA prior to the functionalization of AuNPs provided an LOD of 0.4 nM (20 ng/mL). This LOD in combination with a short incubation time (3 h) was comparable to many other detection assays.[8,13] Additionally, the steric constraints induced by the AuNPs could be eliminated by employing the indirect assay. However, one more step of sample preparation was required for this assay. In order to further reduce the assay time and simplify the procedure, strategy B was performed. The bibiotinylated peptide **2** was incubated with the BoLcA sample and subsequently mixed with the navi-AuNPs. This was a simple one-step process with a total assay time of 4 h. The LOD of this method was 0.1 nM, that is 50-fold lower as compared to the direct mixing assay (A). The reproducibility of the assays reported herein can be considered to be good based on the standard deviations for the experiments presented in Figure 4 (panels b and d) and Figure 5b, given that they rely on experiments undertaken during a time span of several months.

The detection is actually reporting the activity rather than the amount of BoLcA, which is more valuable in sensing applications due to the crucial role played by the proteolytic function of botulinum neurotoxins. In addition, the specificity is ensured by employing peptides designed specifically for BoLcA recognition and catalytic cleavage based on the actual BoNT substrate.[9] Importantly, here the aggregation state of the particles is inversely related to the activity of BoLcA. This inverse relation also effectively reduces the possibility of false positives. Taken together, the colorimetric detection method described herein provides an attractive alternative for the detection of other serotypes of botulinum neurotoxins, other types of proteolytic toxins, or even multidetection by the modification of the peptide sequence.

The sensitivity and assay time can probably be improved by optimizing the peptide substrate to make it more accessible to the analyte. It is also possible to improve the sensitivity and LOD by varying the concentration of AuNPs. Experiments along this line have been explored for another system (Troponin I detection using peptide-decorated spherical nanoparticles), and we observed that lowering the concentration of AuNPs offered a slightly improved LOD. However, the dynamic range was reduced upon lowering the concentration of AuNPs. Thus, there is a trade off between LOD and dynamic range that needs to be taken into account when optimizing the AuNP assays. Due to the minor improvement in LOD for the Troponin I system, we have not specifically studied the effect of different concentrations of AuNPs in the presently employed assay formats. Finally, we believe that the presented BoLcA detection strategies offer a good opportunity for the integration of colorimetric assays into a lateral flow device or a paper-based format for point-of-care and field applications.

ASSOCIATED CONTENT

Supporting Information

Additional experimental details as described in text. This material is available free of charge via the Internet at http://pubs.acs.org.

AUTHOR INFORMATION

Corresponding Authors

*E-mail: danai@ifm.liu.se. Tel: +46 13 282616.
*E-mail: bliedberg@ntu.edu.sg. Tel: +65 6316 2957.

Present Address

[†]Division of Molecular Physics, Department of Physics, Chemistry and Biology, Linköping University, 58183 Linköping, Sweden.

Author Contributions

The manuscript was written through contributions of all authors. All authors have given approval to the final version of the manuscript.

Notes

The authors declare no competing financial interest.

ACKNOWLEDGMENTS

This research is supported by the Science & Engineering Research Council (SERC) of Agency for Science, Technology and Research (A*STAR), for projects under the numbers of 102 152 0015. D.A. also acknowledges support from the Swedish Research Council (VR), the Swedish Foundation for Strategic Research (SSF), the Knut and Alice Wallenberg Foundation (KAW), and the Centre in Nano science and technology (CeNano).

REFERENCES

(1) Montecucco, C.; Molgo, J. *Curr. Opin. Pharmacol.* **2005**, *5*, 274−279.
(2) Singh, B. R. *Neurotoxic. Res.* **2006**, *9*, 73−92.
(3) Schiavo, G.; Matteoli, M.; Montecucco, C. *Physiol. Rev.* **2000**, *80*, 717−766.
(4) Li, L.; Singh, B. R. *J. Toxicol., Toxin Rev.* **1999**, *18*, 95−112.
(5) Foran, P. G.; Mohammed, N.; Lisk, G. O.; Nagwaney, S.; Lawrence, G. W.; Johnson, E.; Smith, L.; Aoki, K. R.; Dolly, J. O. *J. Biol. Chem.* **2003**, *278*, 1363−1371.
(6) Arnon, S. S.; Schechter, R.; Inglesby, T. V.; Henderson, D. A.; Bartlett, J. G.; Ascher, M. S.; Eitzen, E.; Fine, A. D.; Hauer, J.; Layton,

M.; Lillibridge, S.; Osterholm, M. T.; O'Toole, T.; Parker, G.; Perl, T. M.; Russell, P. K.; Swerdlow, D. L.; Tonat, K.; Biodefense, W. G. C. *J. Am. Med. Assoc.* **2001**, *285*, 1059−1070.
(7) Koirala, J.; Basnet, S. *Infections in Medicine* **2004**, *21*, 284−289.
(8) Cai, S.; Singh, B. R.; Sharma, S. *Crit. Rev. Microbiol.* **2007**, *33*, 109−125.
(9) Turton, K.; Chaddock, J. A.; Acharya, K. R. *Trends Biochem. Sci.* **2002**, *27*, 552−558.
(10) Kalb, S. R.; Smith, T. J.; Moura, H.; Hill, K.; Lou, J. L.; Geren, I. N.; Garcia-Rodriguez, C.; Marks, J. D.; Smith, L. A.; Pirkle, J. L.; Barr, J. R. *Int. J. Mass Spectrom.* **2008**, *278*, 101−108.
(11) Schmidt, J. J.; Stafford, R. G. *Appl. Environ. Microbiol.* **2003**, *69*, 297−303.
(12) Marconi, S.; Ferracci, G.; Berthomieu, M.; Kozaki, S.; Miquelis, R.; Boucraut, J.; Michael, S. B.; Leveque, C. *Toxicol. Appl. Pharmacol.* **2008**, *233*, 439−446.
(13) Sapsford, K. E.; Granek, J.; Deschamps, J. R.; Boeneman, K.; Blanco-Canosa, J. B.; Dawson, P. E.; Susumu, K.; Stewart, M. H.; Medintz, I. L. *ACS Nano* **2011**, *5*, 2687−2699.
(14) Ghadiali, J. E.; Stevens, M. M. *Adv. Mater.* **2008**, *20*, 4359−4363.
(15) Rosi, N. L.; Mirkin, C. A. *Chem. Rev.* **2005**, *105*, 1547−1562.
(16) Wilson, R. *Chem. Soc. Rev.* **2008**, *37*, 2028−2045.
(17) Aili, D.; Stevens, M. M. *Chem. Soc. Rev.* **2010**, *39*, 3358−3370.
(18) Aili, D.; Enander, K.; Rydberg, J.; Nesterenko, I.; Bjorefors, F.; Baltzer, L.; Liedberg, B. *J. Am. Chem. Soc.* **2008**, *130*, 5780−5788.
(19) Slocik, J. M.; Zabinski, J. S.; Phillips, D. M.; Naik, R. R. *Small* **2008**, *4*, 548−551.
(20) Aili, D.; Mager, M.; Roche, D.; Stevens, M. M. *Nano Lett.* **2011**, *11*, 1401−1405.
(21) Aili, D.; Selegard, R.; Baltzer, L.; Enander, K.; Liedberg, B. *Small* **2009**, *5*, 2445−2452.
(22) Chen, P.; Selegård, R.; Aili, D.; Liedberg, B. *Nanoscale* **2013**, *5*, 8973−8976.
(23) Laromaine, A.; Koh, L. L.; Murugesan, M.; Ulijn, R. V.; Stevens, M. M. *J. Am. Chem. Soc.* **2007**, *129*, 4156−4157.
(24) Wang, Z.; Levy, R.; Fernig, D. G.; Brust, M. *J. Am. Chem. Soc.* **2006**, *128*, 2214−2215.
(25) Guarise, C.; Pasquato, L.; De Filippis, V.; Scrimin, P. *Proc. Natl. Acad. Sci. U.S.A.* **2006**, *103*, 3978−3982.
(26) Gupta, S.; Andresen, H.; Ghadiali, J. E.; Stevens, M. M. *Small* **2010**, *6*, 1509−1513.
(27) Schmidt, J. J.; Bostian, K. A. *J. Protein Chem.* **1995**, *14*, 703−708.
(28) Schmidt, J. J.; Bostian, K. A. *J. Protein Chem.* **1997**, *16*, 19−26.
(29) Blasi, J.; Chapman, E. R.; Link, E.; Binz, T.; Yamasaki, S.; Decamilli, P.; Sudhof, T. C.; Niemann, H.; Jahn, R. *Nature* **1993**, *365*, 160−163.
(30) Read, T.; Olkhov, R. V.; Shaw, A. M. *Phys. Chem. Chem. Phys.* **2013**, *15*, 6122−6127.
(31) Hermanson, G. T. *Bioconjugate Techniques*, 2nd ed.; Academic Press: Waltham, MA, 2008.
(32) Marttila, A. T.; Laitinen, O. H.; Airenne, K. J.; Kulik, T.; Bayer, E. A.; Wilchek, M.; Kulomaa, M. S. *FEBS Lett.* **2000**, *467*, 31−36.
(33) Kukreja, R.; Singh, B. R. In *Microbial Toxins: Current Research and Future Trends*; Caister Academic Press: Norfolk, England, U.K., 2009.
(34) Breidenbach, M. A.; Brunger, A. T. *Nature* **2004**, *432*, 925−929.
(35) Ladd, J.; Taylor, A. D.; Homola, J.; Jiang, S. Y. *Sens. Actuators, B* **2008**, *130*, 129−134.
(36) Lindstrom, M.; Korkeala, H. *Clin. Microbiol. Rev.* **2006**, *19*, 298−314.
(37) Poli, M. A.; Rivera, V. R.; Neal, D. *Toxicon* **2002**, *40*, 797−802.
(38) Szilagyi, M.; Rivera, V. R.; Neal, D.; Merrill, G. A.; Poli, M. A. *Toxicon* **2000**, *38*, 381−389.
(39) Wei, F.; Ho, C. M. *Anal. Bioanal. Chem.* **2009**, *393*, 1943−1948.